

NOT THE PUBLISHED VERSION; this is the author's final, peer-reviewed manuscript. The published version may be accessed by following the link in the citation at the bottom of the page.

The *dapE*-encoded *N*-Succinyl-*l,l*-Diaminopimelic Acid Desuccinylase from *Haemophilus influenzae* Is a Dinuclear Metallohydrolase

Nathaniel J. Coper

*Department of Chemistry, University of Georgia,
Athens, GA*

David L. Bienvenue

*Department of Chemistry and Biochemistry,
Utah State University,
Logan, UT*

Jacob E. Shokes

*Department of Chemistry, University of Georgia,
Athens, GA*

Danuta M. Gilner

*Department of Chemistry and Biochemistry,
Utah State University,
Logan, UT*

Takashi Tsukamoto

*Guilford Pharmaceuticals Inc.,
Baltimore, MD*

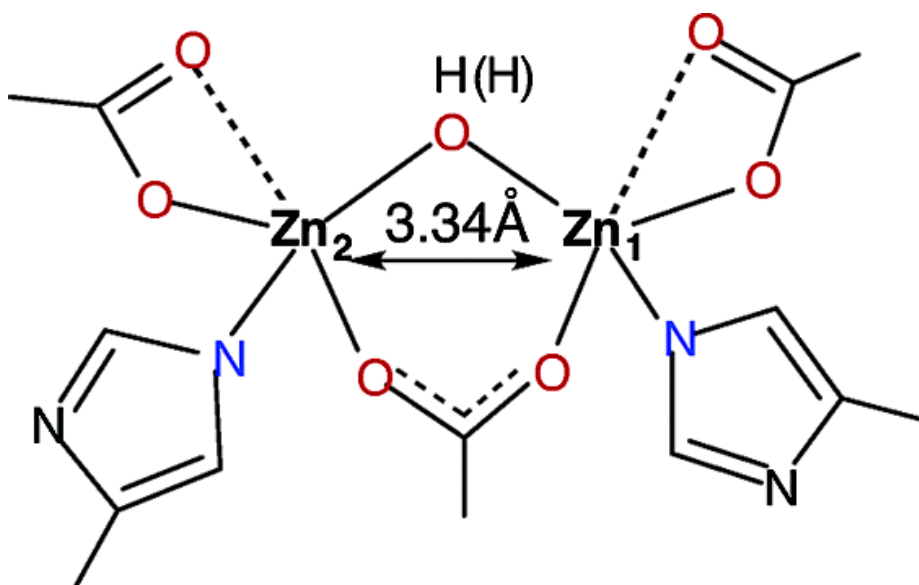
Robert A. Scott

Department of Chemistry, University of Georgia,
Athens, GA

Richard C. Holz

Department of Chemistry and Biochemistry,
Utah State University,
Logan, UT

Abstract



The Zn K-edge extended X-ray absorption fine structure (EXAFS) spectra, of the *dapE*-encoded *N*-succinyl-L,L-diaminopimelic acid desuccinylase (DapE) from *Haemophilus influenzae* have been recorded in the presence of one or two equivalents of Zn(II) (i.e. [Zn_(DapE)] and [ZnZn(DapE)]). The Fourier transforms of the Zn EXAFS are dominated by a peak at ca. 2.0 Å, which can be fit for both [Zn_(DapE)] and [ZnZn(DapE)], assuming ca. 5 (N,O) scatterers at 1.96 and 1.98 Å, respectively. A second-shell feature at ca. 3.34 Å appears in the [ZnZn(DapE)] EXAFS spectrum but is significantly diminished in [Zn_(DapE)]. These data show that DapE contains a dinuclear Zn(II) active site. Since no X-ray crystallographic data are available for any DapE enzyme, these data provide the first glimpse at the active site of DapE enzymes. In addition, the EXAFS data for DapE incubated with two competitive inhibitors,

2-carboxyethylphosphonic acid and 5-mercaptopentanoic acid, are also presented.

According to recent estimates from the United States Centers for Disease Control and Prevention (the CDC), more than 10 million people died worldwide from bacterial infections in 1995.¹ Tuberculosis, for example, was the leading cause of death in adults by an infectious disease.² The importance of developing new drugs to fight infectious disease, such as tuberculosis, is underscored by the emergence of several pathogenic bacterial strains that are resistant to all currently available antibiotics.³⁻⁶ To overcome bacterial resistance to antibiotics, new enzyme targets must be located and small-molecule inhibitors developed. The *meso*-diaminopimelate (mDAP)/lysine biosynthetic pathway offers several potential anti-bacterial targets that have yet to be explored.⁷⁻⁹ Since both products of this pathway, mDAP and lysine, are essential components of the peptidoglycan cell wall in Gram-negative and some Gram-positive bacteria, inhibitors of enzymes within this pathway may provide a new class of antibiotics.⁵ The fact that there are no similar pathways in mammals suggests that inhibitors of enzymes in the mDAP/lysine pathway will provide selective toxicity against bacteria and will potentially have little or no effect on humans.

One of the enzymes in this pathway,¹⁰ the *dapE*-encoded *N*-succinyl-L,L-diaminopimelic acid desuccinylase (DapE), catalyzes the hydrolysis of *N*-succinyl-L,L-diaminopimelate to L,L-diaminopimelate and succinate.¹¹ It has been shown that deletion of the gene encoding DapE is lethal to *Helicobacter pylori* and *Mycobacterium smegmatis*.^{12,13} Even in the presence of lysine-supplemented media, the DapE deletion cell line of *H. pylori* was unable to grow. Therefore, DapEs are essential for cell growth and proliferation. Since no structural data of any kind are available for DapE enzymes, we have recorded the Zn K-edge extended X-ray absorption fine structure (EXAFS) spectra of the DapE from *H. influenzae* in the presence of one or two equivalents of Zn(II) (i.e. [Zn_(DapE)] and [ZnZn(DapE)]) (Figure 1). For [ZnZn(DapE)] the EXAFS data report an average of both metal ion environments. The Fourier transforms of both [Zn_(DapE)] and [ZnZn(DapE)] are dominated by a peak at ca. 2.0 Å, that can be fit for both [Zn_(DapE)] and [ZnZn(DapE)] assuming 5 (N,O) scatterers, at 1.96 and 1.98 Å, respectively (Fits 1,3; Table 1). A

second shell feature at ca. 3.3 Å appears in the [ZnZn(DapE)] EXAFS spectrum but is significantly diminished in [Zn_(DapE)]. Fits incorporating a Zn–Zn interaction at 3.34 Å for [ZnZn(DapE)] have reasonable Debye–Waller factors (Fit 4; Table 1) and resulted in a significant improvement in goodness-of-fit values (f'). Therefore, the second-shell FT feature observed at 3.34 Å is consistent with a dinuclear Zn(II) active site in DapE. Although fits for [Zn_(DapE)] that include a Zn–Zn interaction improve the f' values slightly, the Debye–Waller factor value for this interaction is significantly higher than for the same interaction in [ZnZn(DapE)] (cf. Fits 2,4; Table 1).

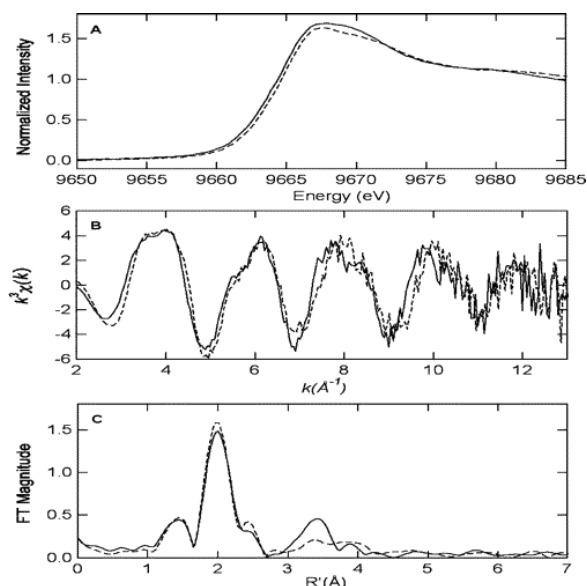


Figure 1 Zn K-edge X-ray absorption spectra for [Zn_(DapE)] (dashed) and [ZnZn(DapE)] (solid). (A) Zn edge spectra; (B) k^3 -weighted Zn EXAFS; (C) Fourier transforms over $k = 2\text{--}13 \text{ Å}^{-1}$, with S phase correction.

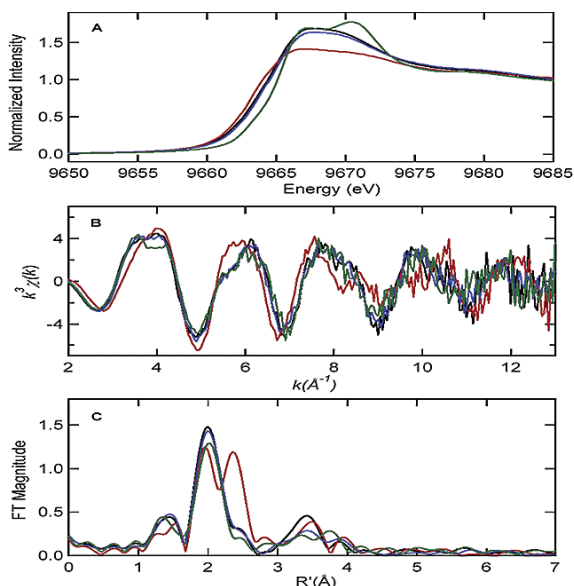


Figure 2 Zn K-edge X-ray absorption spectra of [ZnZn(DapE)] in the absence (black) and presence of CEPA (blue) or MSPA (red) and [ZnZn(APP)] in the presence of LPA (green). (A) Zn edge spectra; (B) k^3 -weighted Zn EXAFS; (C) Fourier transforms over $k = 2\text{--}13 \text{ \AA}^{-1}$, with S phase correction.

Table 1. Curve-Fitting Results for Zn EXAFS^a of DapE Enzymes

sample filename (k range) $\Delta k^3\chi$	fit	shell	R_{as} (Å)	σ_{as}^2 (Å ²)	ΔE_0 (eV)	f^b
[Zn_(DapE)]	1	Zn–O ₅	1.96	0.0062	–9.11	0.104
ZDZ0A (2–13 Å ⁻¹)	2	Zn–O ₅	1.96	0.0062	–9.30	0.100
$\Delta k^3\chi = 10.23$		Zn–Zn	3.30	0.0117		
[ZnZn(DapE)]	3	Zn–O ₅	1.98	0.0065	–9.01	0.111
ZDZ0A (2–13 Å ⁻¹)	4	Zn–O ₅	1.98	0.0064	–9.41	0.093
$\Delta k^3\chi = 10.44$		Zn–Zn	3.34	0.0051		
[ZnZn(AAP)]	5	Zn–O ₅	1.99	0.0084	–8.71	0.094
ZAZZA (2–13 Å ⁻¹)	6	Zn–O ₅	1.99	0.0084	–9.12	0.089
$\Delta k^3\chi = 9.47$		Zn–Zn	3.27	0.0099		
[ZnZn(DapE)]-CEPA	7	Zn–O ₅	1.99	0.0069	–8.00	0.096
ZDZ0A (2–13 Å ⁻¹)	8	Zn–O ₅	1.99	0.0085	–8.42	0.088
$\Delta k^3\chi = 9.89$		Zn–Zn	3.34	0.0083		
[ZnZn(AAP)]-LPA	9	Zn–O ₅	1.99	0.0078	–8.22	0.108
ZAZPA (2–13 Å ⁻¹)	10	Zn–O ₅	1.99	0.0077	–8.56	0.103
$\Delta k^3\chi = 9.91$		Zn–Zn	3.30	0.0112		
	11	Zn–O ₅	1.99	0.0077	–8.49	0.103
		Zn–Zn	3.80	0.0072		
[ZnZn(DapE)]-MSPA	12	Zn–O ₅	1.99	0.0079	–3.03	0.109
ZDZTA (2–13 Å ⁻¹)	13	Zn–O ₅	1.99	0.0050	–6.24	0.097
$\Delta k^3\chi = 9.98$		Zn–S	2.30	0.0089		
		Zn–Zn	3.64	0.0083		

^a Shell is the chemical unit defined for the multiple scattering calculation, the number of scatterers per metal denoted by the subscript. R_{as} is the metal-scatterer distance. σ_{as}^2 is a mean square deviation in R_{as} . ΔE_0 is the shift in E_0 for the theoretical scattering functions.^b f^{χ} is a normalized error (χ -squared): $f^{\chi} = \{\sum_i [k^3(-)]^2/N\}^{1/2}/[(k^3\chi^{obs})_{max} - (k^3\chi^{obs})_{min}]$.

Sequence alignments of several DapE genes with those of the crystallographically characterized aminopeptidase from *Aeromonas proteolytica* (AAP) and the carboxypeptidase G₂ from *Pseudomonas* sp. strain RS-16 (CPG₂), indicate that all of the amino acids that function as metal ligands in AAP and CPG₂ are strictly conserved in DapEs.^{11,14-16} The X-ray crystal structures of both CPG₂ and AAP reveal a (μ -aquo)(μ -carboxylato)dizinc(II) active site with one terminal carboxylate and histidine residue bound to each metal ion.^{15,16} Both Zn(II) ions in AAP and CPG₂ reside in a distorted tetrahedral coordination geometry, with a Zn–Zn distance of 3.5 and 3.3 Å for AAP and CPG₂, respectively.^{15,16} EXAFS data obtained for [ZnZn(AAP)] also contain a feature at 3.27 Å that can be modeled as a Zn–Zn vector (Fit 6; Table 1). Combination of these data indicates that DapE enzymes contain dinuclear Zn(II) active sites. In addition, on the basis of the first shell fits of [ZnZn(AAP)] and [ZnZn(DapE)], we propose that one carboxylate and one histidine residue resides at each Zn(II) site in DapE and that the two Zn(II) ions are bridged by one carboxylate residue and a water molecule.

The first step in inhibitor design for DapE enzymes requires an understanding of how inhibitors bind to the active site. Therefore, we recorded the Zn K-edge EXAFS spectra of [ZnZn(DapE)] in the presence of the competitive inhibitors 2-carboxyethylphosphonic acid (CEPA) and 5-mercaptopentanoic acid (MSPA) (Figure 2). The EXAFS data for [ZnZn(DapE)]–CEPA indicate that the average coordination number of each Zn(II) ion remains five and the Zn–Zn distance remains 3.34 (Fits 7,8; Table 1). An increase in the M–M distance of [ZnZn(AAP)], from 3.5 to 3.9 Å, is observed upon the addition of the transition-state analogue inhibitor l-leucine-phosphonic acid (LPA) which contains a similar ligating group to CEPA.¹⁷ The X-ray crystal structure and EXAFS data for [ZnZn(AAP)]–LPA, reveal that the bridging water molecule is displaced by LPA resulting in an η -1,2- μ -phosphonate bridge and an increase in the Zn–Zn distance of 0.4 Å (Fit 11; Table 1). The fact that the Zn–Zn distance does not change upon CEPA binding to [ZnZn(DapE)] suggests an η -1- μ -phosphonate

bridge exists, similar to the binding mode of LPA to the leucine aminopeptidase from bovine lens.^{17,18} On the other hand, MSPA binding to [ZnZn(DapE)] has a marked effect on the Zn K-edge, suggesting that the average electronic environment of the dinuclear Zn(II) site has changed significantly (Figure 2). The observed shift to lower energy in the absorption edge position is indicative of a net increase in electron density at the dinuclear Zn(II) site, consistent with a sulfur ligand. In addition, the EXAFS data for [ZnZn(DapE)]–MSPA reveal a new feature at 2.3 Å that is highly characteristic of a direct zinc–sulfur interaction (Fits 12,13; Table 1). Moreover, the M–M distance is lengthened from 3.34 to 3.64 Å. These data indicate that the thiol group of MSPA binds to one or more of the Zn(II) ions in the active site of DapE.

In conclusion, DapEs are potential molecular targets for a new and novel class of antibiotics. The EXAFS data presented herein provide the first structural information for any DapE enzyme and also establish the binding modes of phosphonate- and thiolate-containing inhibitors. In addition, the structural data obtained for CEPA bound to [ZnZn(DapE)] provide the first glimpse at the transition state of the hydrolysis reaction catalyzed by DapE. Since most pharmaceuticals target the transition state of enzymatic reactions, the structural aspects of [ZnZn(DapE)]–CEPA are particularly important for the rational design of new potent inhibitors of DapE enzymes.

Acknowledgment

This work was supported by the National Institutes of Health (GM-42025, R.A.S.) and the National Science Foundation (CHE-0240810, R.C.H.). The *E. coli* BL21(DE3) strain expressing the recombinant *H. influenzae* dapE-encoded desuccinylase was provided by Professor John S. Blanchard (Albert Einstein College of Medicine, supported by AI-33696).

Supporting Information Available

Experimental details (PDF). This material is available free of charge via the Internet at <http://pubs.acs.org>.

References

- ¹Henery, C. M. *Chem. Eng. News* **2000**, 41–58.
- ²Snider, D. E.; Raviglione, M.; Kochi, A. In *Global Burden of Tuberculosis*; Bloom, B. R., Ed.; ASM Press: Washington, DC, 1994; pp 3–11.
- ³Prevention. Centers for Disease Control and Prevention: Washington, DC. *MMWR Morb. Mortal. Wkly Rep.* **1995**, *44*, 1–13.
- ⁴Howe, R. A.; Bowker, K. E.; Walsh, T. R.; Feest, T. G.; MacGowan, A. P. *Lancet* **1997**, *351*, 601–602.
- ⁵Levy, S. B. *Sci. Am.* **1998**, *278*, 46–53.
- ⁶Chin, J. *New Sci.* **1996**, *152*, 32–35.
- ⁷Scapin, G.; Blanchard, J. S. *Adv. Enzymol.* **1998**, *72*, 279–325.
- ⁸Born, T. L.; Blanchard, J. S. *Curr. Opin. Chem. Biol.* **1999**, *3*, 607–613.
- ⁹Girodeau, J.-M.; Agouridas, C.; Masson, M.; R., P.; LeGoffic, F. *J. Med. Chem.* **1986**, *29*, 1023–1030.
- ¹⁰Velasco, A. M.; Leguina, J. I.; Lazcano, A. *J. Mol. Evol.* **2002**, *55*, 445–459.
- ¹¹Born, T. L.; Zheng, R.; Blanchard, J. S. *Biochemistry* **1998**, *37*, 10478–10487.
- ¹²Karita, M.; Etterbeek, M. L.; Forsyth, M. H.; Tummuru, M. R.; Blaser, M. J. *Infect. Immun.* **1997**, *65*, 4158–4164.
- ¹³Pavelka, M. S.; Jacobs, W. R. *J. Bacteriol.* **1996**, *178*, 6496–6507.
- ¹⁴Makarova, K. S.; Grishin, N. V. *J. Mol. Biol.* **1999**, *292*, 11–17.
- ¹⁵Chevrier, B.; Schalk, C.; D'Orchymont, H.; Rondeau, J.-M.; Moras, D.; Tarnus, C. *Structure* **1994**, *2*, 283–291.
- ¹⁶Rowell, S.; Pauptit, R. A.; Tucker, A. D.; Melton, R. G.; Blow, D. M.; Brick, P. *Structure* **1997**, *5*, 337–347.
- ¹⁷Stamper, C.; Bennett, B.; Edwards, T.; Holz, R. C.; Ringe, D.; Petsko, G. *Biochemistry* **2001**, *40*, 7034–7046.
- ¹⁸Sträter, N.; Lipscomb, W. N. *Biochemistry* **1995**, *34*, 9200–9210.